Biomaterials 29 (2008) 4575–4583

Contents lists available at ScienceDirect

Biomaterials

journal homepage: www.elsevier.com/locate/biomaterials

# Notched stress–strain behavior of a conventional and a sequentially annealed highly crosslinked UHMWPE

Michael C. Sobieraj [a,b], Steven M. Kurtz [c], A. Wang [d], Michael M. Manley [e], Clare M. Rimnac [a,b,*]

[a] Musculoskeletal Mechanics and Materials Laboratories, Department of Mechanical and Aerospace Engineering, Case Western Reserve University, Cleveland, OH, USA
[b] Department of Orthopaedics, Case Western Reserve University, Cleveland, OH, USA
[c] Drexel University and Exponent, Inc., Philadelphia, PA, USA
[d] Stryker Orthopaedics, Mahwah, NJ, USA
[e] Homer Stryker Center for Orthopaedic Education, Mahwah, NJ, USA

ARTICLE INFO

*Article history:*
Received 25 June 2008
Accepted 20 August 2008
Available online 17 September 2008

*Keywords:*
UHMWPE
Notch
Crosslinking
Tensile properties

ABSTRACT

Contemporary total joint replacement designs contain stress-risers such as fillets, grooves, and undercuts; therefore, it is of interest to analyze the behavior of UHMWPEs in the presence of such design-related stress-risers. This study examined the engineering and true axial stress–strain behavior of smooth cylindrical and notched cylindrical test specimens, under applied axial tensile loading (2 displacement rates, 37 °C) for a conventional and a highly crosslinked second generation UHMWPE. Both materials were prepared from ram extruded GUR 1050. The conventional material (30 kGy) was gamma sterilized at 30 kGy in an inert $N_2$ environment. The sequentially annealed material (SA) was gamma irradiated at 30 kGy and annealed for 8 h at 130 °C. The irradiation-annealing process was repeated two more times for an overall irradiation dose of 90 kGy. Differential scanning calorimetry (DSC) was utilized to investigate changes in crystallinity and lamellar thickness distributions upon loading. Fractographic analysis of scanning electron microscope (SEM) images of fracture surfaces was performed to investigate changes in fracture micromechanism with notching. Both the 30 kGy and SA materials, in the smooth condition, demonstrated substantial ductility and orientation hardening. With the introduction of a notch, both materials demonstrated an elevation in the yield stress (notch strengthening) and a reduction in the ultimate stress and ultimate strain at both displacement rates. Additionally, it was found that the uniaxial stress-state (smooth condition) allowed for greater changes in crystallinity and the lamellar thickness distributions, when compared to the untested materials, than the triaxial stress-state induced by the notched geometry.



## 1. Introduction

For almost four decades ultra-high molecular weight polyethylene (UHMWPE) has been used for bearing component of total joint replacements (TJR). Over one million people a year are treated for various joint problems with TJRs that use UHMWPE as the bearing material. Projections show increasing numbers of younger, more active, patients receiving TJRs, necessitating longer performance of these devices [1,2].

Wear of UHMWPE components is a significant problem due to formation of UHMWPE debris that can cause a biological cascade of events leading to bone resorption and periprosthetic osteolytic implant loosening [3]. To combat this wear problem, crosslinking, using ionizing radiation was reintroduced in the 1990s [4] with precautions taken to reduce the amount of residual free radicals generated in the crosslinking process. Both remelting, done above, and annealing, done below the peak melt temperature ($T_m$), have been used to combat residual free radicals. Remelting is highly effective at eliminating free radicals [5], but has been shown to decrease crystallinity and lamellar thickness resulting in a decrease in yield stress, ultimate stress, and fatigue crack propagation resistance [4,6]. Annealing does not adversely affect crystallinity [4,6], but does leave some free radicals, which can lead to oxidative degradation of the material [7,8].

Sequential irradiation and annealing has been introduced as a means by which to more effectively reduce free radicals without remelting the material and without adverse changes in crystallinity [9,10]. Sequentially irradiated and annealed UHMWPE has shown promising results in mechanical and aging studies [9,10]. X3™ (Stryker Orthopaedics, Mahwah, NJ) is currently the only sequentially irradiated annealed UHMWPE on the market.

* Corresponding author. Tel.: +1 216 368 6442; fax: +1 216 368 3007.
*E-mail address:* clare.rimnac@case.edu (C.M. Rimnac).

0142-9612/$ – see front matter © 2008 Elsevier Ltd. All rights reserved.
doi:10.1016/j.biomaterials.2008.08.010

Implant designs contain stress-risers such as fillets, grooves, and undercuts. Therefore, it is of interest to analyze the behavior of UHMWPEs in the presence of design-related stress-risers. Notched monotonic tensile tests of conventional and highly crosslinked UHMWPEs demonstrated that the triaxial stress state induced by the notch resulted in an elevation of axial yield stress (a phenomenon known as notch strengthening), a decrease in orientation hardening, and a change in the fracture micromechanism [11].

The purpose of this study was to investigate the effects of notching and displacement rate on the material properties, notch strengthening, orientation hardening, fracture micromechanism, and concomitant changes in the crystalline regions upon deformation for a conventional and a sequentially annealed UHMWPE. We hypothesized that the sequentially annealed UHMWPE would show notch strengthening, a truncation of orientation hardening, and a change in fracture micromechanism upon notching.

## 2. Materials and methods

### 2.1. Mechanical properties

Two UHMWPE materials made from ram extruded GUR 1050 were examined. The conventional material (30 kGy) was gamma sterilized at 30 kGy in an inert $N_2$ environment. The sequentially annealed material (SA) was gamma irradiated at 30 kGy and annealed for 8 h at 130 °C. The irradiation-annealing process was repeated two more times for an overall irradiation dose of 90 kGy; this approximated the process used by Stryker Orthopaedics to make X3™.

Smooth specimens and notched specimens 100 mm in total length were machined (Fig. 1). The smooth specimens had a gauge diameter of 8 mm, with a tested gauge length of 10 mm. The notched specimens had an outer 8 mm and an inner diameter of 6 mm with a 0.45 mm notch radius (elastic stress concentration factor: $k_t = 2.69$).

Specimens were soaked for 8 weeks in phosphate buffered saline at 37 °C then monotonically loaded to failure in air at 37 °C (4411 electromechanical frame, Instron, Canton, MA). Tests were conducted at both 30 mm/min and 150 mm/min. For each material, notch condition, and rate 14 ± 2 specimens were tested (116 total specimens).

Smooth specimen engineering strain was obtained using a non-contacting video extensometer (Instron, Canton, MA). For the notched specimens, engineering strain was obtained using a previously developed non-contacting video based method [11]. Custom written MATLAB programs were used for the generation of both engineering and true stress strain curves [11].

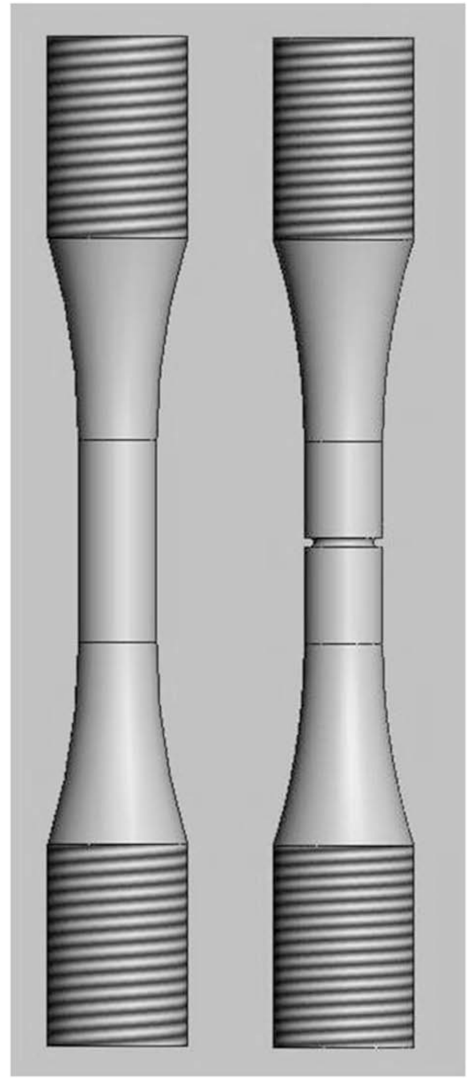

**Fig. 1.** Illustration of the two geometries of specimens used in this study. Left: smooth; Right: notched.

### 2.2. Notch strengthening and hardening ratios

For each of the specimens, a notch strengthening ratio was calculated:

$$\varphi_\sigma = \frac{\sigma_y}{\overline{\sigma_{y,\text{smooth}}|_{\text{rate}}}} \tag{1}$$

where $\varphi_\sigma$ is the notch strengthening ratio, $\sigma_y$ is the true yield stress of an individual specimen and $\overline{\sigma_{y,\text{smooth}}}$ is the mean true yield stress of the smooth specimens tested at the same displacement rate.

A hardening ratio was also calculated for each of the specimens:

$$\psi_\sigma = \frac{\sigma_u}{\sigma_y} \tag{2}$$

where $\psi_\sigma$ is the hardening ratio, $\sigma_u$ is the true ultimate stress, and $\sigma_y$ is the true yield stress for a specimen.

### 2.3. Crystallinity and lamellar thickness distributions

To examine the effect of deformation on crystallinity, differential scanning calorimetry (DSC, Mettler-Toledo DSC 823e, Columbus, OH) was performed on 5 specimens from each of the 8 possible material–geometry–rate combinations as well as for each of the two undeformed materials (60 total DSC crystallinity samples). The samples, approximately 5 mg, were cut from the notched region (notched samples) or from the gauge region directly adjacent to the fracture surface (smooth samples).

Samples were brought to thermal equilibrium at 25 °C and then heated at 10 °C/min to 180 °C. Crystallinity was then calculated using the heat of fusion of a perfect crystal of polyethylene ($\Delta H_f$, 289.3 J/g), and the area under the curve between 50 °C and 160 °C ($\Delta H_m$) [12,13].

$$\text{Crystallinity} = \frac{\Delta H_m}{\Delta H_f} \tag{3}$$

Additionally, lamellar thickness (LT) distributions of the crystalline regions were calculated. One sample, approximately 10 mg, was cut from one specimen from each of the eight material–geometry–rate combinations and from the two undeformed conditions. The samples were heated from 50 °C to 180 °C at 1 °C/min following Stephens et al. [14]. The probability distribution function of lamellar thicknesses, $g(l)$, was found by plotting $g(T)$, mass fraction of crystals melting at a given temperature, vs $l(T)$, lamellar thickness based on the Gibbs equation, as shown in Eqs. (4a) and (4b)[12,15].

$$g(T) = KP(T)(T_{m0} - T)^2 \tag{4a}$$

$$l(T) = \frac{2\sigma_e}{\Delta H_v}\frac{T_{m0}}{(T_{m0} - T)} \tag{4b}$$

$P(T)$ is the corrected DSC curve, $\sigma_e = 93 \times 10^{-7}$ J/cm$^2$ (fold surface energy), $\Delta H_v = 280$ J/cm$^3$ (heat of fusion of crystalline PE), and $T_{m0} = 418.7$ K (equilibrium melting temperature) [12].

### 2.4. Fracture micromechanism

One fracture surface from each tested specimen was sputter coated with palladium and then documented photographically via stereomicroscopy. The fractures of the notched specimens either exhibited one or two distinct fracture zones (inner and outer zones); when present, the ratio of the radii of the inner zone to that of the entire fracture surface was calculated. A representative fracture surface from each of the eight material–geometry–rate combinations was also examined using scanning electron microscopy (SEM, Hitachi S-4500, Tokyo Japan) at 5 kV.